ELSEVIER

Journal of Photochemistry and Photobiology A: Chemistry 96 (1996) 109–121

Journal of PHOTOCHEMISTRY AND PHOTOBIOLOGY A: CHEMISTRY

Matrix and temperature effects on absorption spectra of β-carotene and pheophytin *a* in solution and in green plant photosystem II

I. Renge [1] *, R. van Grondelle, J.P. Dekker

Department of Physics and Astronomy, Institute of Molecular Biological Sciences, Vrije Universiteit, De Boelelaan 1081, 1081 HV Amsterdam, Netherlands

Received 27 September 1995; accepted 9 January 1996

Abstract

Absorption spectra of β-carotene (β-Car) and pheophytin (Pheo) *a* have been recorded in a number of solvents and polymers and the properties are compared with those observed in the isolated reaction centre complex of green plant photosystem II and in its core antenna complex CP47. The peak maxima of the investigated absorption bands shift to the red with increasing polarizability of the medium. The extent of the shift is in the order β-Car > Pheo (Soret) > Pheo (Q_x) > Pheo (Q_y), and it exhibits a linear relationship with the Lorentz–Lorenz function $(n^2-1)/(n^2+2)$ of the refractive index of the solvent. The maxima also depend on the polarity of the solvent, and for liquids with similar refractive indices the shift in the maxima of the absorption bands was found to be proportional to the dielectric permittivity function $(\epsilon-1)/(\epsilon+2)$. Most absorption bands shift strongly (β-Car) or weakly (Pheo Soret and Q_x) to the red when the polarity is increased, but the Pheo Q_y band shifts to the blue. All investigated absorption bands also broaden with increasing polarity of the medium. The temperature dependence of the absorption properties was recorded in poly(vinyl butyral) and polystyrene matrices between 80 and 295 K. The purely thermal shift of the absorption maxima was calculated from the difference between the observed shift and the estimated dispersive shift. The thermal and dispersive effects cause in most cases blue and red shifts respectively on cooling, but for β-Car both effects lead to red shifts on cooling from room temperature to 110–160 K. The absorption bands of β-Car in CP47 are remarkably narrow, suggesting a non-polar and highly uniform environment. The temperature-induced band shift is much larger in CP47 than in the polymer matrices, which probably is related to a phase transition of the protein matrix at about 200 K. At room temperature, the effective refractive index of the CP47 host was estimated to be 1.51 ± 0.04. The absorption bands of β-Car in the isolated photosystem II reaction centre complex are distorted because of excitonic interactions but exhibit roughly the same temperature dependence as those in CP47. The Pheo *a* Q_x absorption band is considerably red shifted compared with that in solvents and polymers, which is ascribed to specific interactions with the reaction centre proteins.

Keywords: Absorption; β-Carotene; Pheophytin; Photosystem II; Pigment-proteins; Polymers; Solvent shift; Temperature shift

1. Introduction

It is not a straightforward task to calculate absorption spectra of chlorophylls and carotenoids in native pigment–protein complexes, even for those complexes of which the structure is known in detail [1]. The spectra of the native complexes can, however, be compared with those of isotropic solutions of the isolated pigments in liquids and polymers, which allows one to discern the influence of dielectric and thermal effects and to estimate the pigment–pigment coupling and specific solvation of the protein environment.

For instance, the ability of proteins to coordinate the central Mg atom of chlorophyll *a* (Chl *a*) and to form hydrogen bonds was investigated in solvents containing structural fragments of amino acids [2]. Solvent effects on the absorption maxima of a number of tetrapyrrolic pigments, including Chl *a*, have been reviewed recently in Ref. [3]. Absorption spectra of three carotenoids have been analysed in solutions with different polarizabilities in order to obtain information on their environments in bacterial light-harvesting antenna complexes [4]. In a set of common solvents, the energy of the strongly allowed S_2 transition of lycopene [5] and of all-*trans*-β-carotene [4,6,7] (β-Car) can vary to a rather significant extent (about 1500 cm^{-1} or 40 nm). The wavenumber of the absorption maximum appeared to depend on the refractive index [4,7–9], which was ascribed to a dispersive effect resulting from the high polarizability of the S_2 state [4] or from the large transition moment [8,9]. An analysis of absorption band shapes and Raman excitation profiles of β-Car in terms of vibrational frequencies, Franck–Condon factors and homogeneous and inhomogeneous band-

* Corresponding author.

[1] Permanent address: Institute of Physics, EE2400 Tartu, Estonia.

PII S1010-6030(96)04302-X

widths in liquid and solid matrices at selected temperatures can be found in Refs. [10–13].

As a continuation of these studies, we examined in this work the maxima and the widths of the absorption bands of β-Car and pheophytin *a* (Pheo *a*) in several liquids and polymers and compared the spectral properties with those in pigment–protein complexes of photosystem II (PS II) of higher plants. Despite the fact that photosynthetic pigment–protein complexes from higher plants reveal in general much less spectral resolution than those from photosynthetic purple bacteria, the isolated reaction centre (RC) complex of PS II (the PS II RC complex, also known as the D1–D2–cytochrome *b*-559 complex) shows distinct absorption bands of β-Car and Pheo *a* in the spectral window between the strong $Q_y(S_1)$ and Soret band systems of the chlorophylls and pheophytins [14]. In addition, the intrinsic chlorophyll protein CP47 displays a well-resolved first $1^1B_u \leftarrow 1^1A_g$ band of β-Car [15] (from here on denoted as the S_{20} band).

In this report, special attention is paid to the effect of temperature on the spectral properties of β-Car and Pheo *a*. At low temperatures (below 70 K) much information about the zero-phonon line width has been obtained by the hole-burning technique [16–20], but between 77 K and room temperature there is an obvious gap in the spectroscopic research on pigments. We obtained pure thermal shifts of β-Car and Pheo *a* in polymers and correlated these shifts and broadenings with the change of polarizability on excitation. We also compared the observed shifts with those in the intact PS II RC and CP47 protein complexes.

2. Materials and methods

Solvents (Baker and Aldrich) were used without further purification. β-Car and Chl *a* were obtained from Aldrich and Serva respectively. Pheo *a* was prepared from Chl *a* by adding a drop of 10 M HCl to Chl *a* dissolved in acetone–water. The solution was neutralized with ammonia and Pheo *a* was extracted with diethyl ether. The extract was dried with Na_2SO_4 and evaporated in a flow of dry air. PVB and PSt (average molecular weight, ca. 280 000) were obtained from Aldrich and dissolved in chloroform and benzene respectively. The solution was cast in a Petri dish and dried in a dark cold room. The residual solvent was removed by keeping the films (0.1–0.2 mm thick) overnight under vacuum.

PS II CP47–RC (CP47–D1–D2–cytochrome *b*-559) complexes were prepared from spinach grana membranes by using *n*-dodecyl-β,D-maltoside (DM) [21] and served as starting material for the isolation of the PS II RC complex in DM by using a short Triton X-100 treatment [22] and of the CP47 complex in DM by using an $LiClO_4$–DM treatment [23]. For low temperature measurements the samples were diluted in BTT buffer (20 mM BisTris, 20 mM NaCl, 10 mM $MgCl_2$, 1.5% taurine at pH 6.5) supplemented with 0.03% DM and 70% (by volume) glycerol. The samples were cooled in 1.0 cm Perspex cuvettes in an Oxford N_2 reservoir cryostat (model DN 1704), which was connected to an ITC 4 temperature controller. The temperature was recorded (± 2 K accuracy) with a KTY-10 resistor placed directly in the solution.

Absorption spectra were recorded with a computer-controlled Cary 219 spectrophotometer (slit width, 0.5–1 nm; scan speed, 0.5 nm s^{-1}). Wavelength calibration was performed by using the 416.1, 536.5 and 640.5 nm lines of $HoCl_3$ (0.25 M in 10 mM HCl). The reproducibility of the spectrophotometer was better than 0.05 nm and the corrections did not exceed 0.3 nm. The absorption band maxima were accurate within ± 0.1 nm. The spectrum of β-Car was deconvoluted in gaussian components with the aid of a least-squares fitting program.

3. Results and discussion

3.1. Band shifts in non-polar environment

The wavenumbers of absorption band maxima of β-Car (Table 1) and Pheo *a* (Table 2) were determined in a set of *n*-alkanes from pentane to hexadecane. They can very well be correlated with the Lorentz–Lorenz function $\phi(n^2)$ of the solvent (Figs. 1 and 2):

$$\nu = \nu_0 + p\phi(n^2) \quad (1)$$

$$\phi(n^2) = (n^2-1)/(n^2+2)$$

where n is the refractive index at 20°C for the sodium D line, and ν_0 and p are the regression parameters. The intercept ν_0 and slope p values of solvatochromic plots (Eq. (1)) are given in Table 3.

Extrapolation of the solvent polarizability $\phi(n^2)$ to zero yields frequency values which are close to those ν_0^0 of purely electronic origins of jet-cooled molecules [27]. A meaningful comparison of ν_0^0 and the extrapolated value of ν_0 is possible when the 0–0 band in the condensed phase is well separated from vibronic satellites [27]. Thus, the Q_y and Q_x transitions of bare cold Pheo *a* molecules in vacuum are expected to appear at 659 nm and 524 nm (15 173 cm^{-1} and 19 079 cm^{-1}; see Table 3) respectively. The absorption onset of the B band system in free Pheo *a* should be close to 393 nm (25 413 cm^{-1}).

For β-Car the maximum of the highest peak (labelled as S_{21}) was measured. With the aid of gaussian deconvolution the first band (S_{20}) maximum can be located at 1390 ± 20 cm^{-1} below the S_{21} maximum. The intensity of the purely electronic transition in β-Car is probably small or even negligible, and the S_{20} band is mainly composed of progressions of low frequency modes (see below). Even in this case the intercept ν_0 was found to be very close to the 0–0 origin in cold flexible chromophores, such as tetraphenylporphine, tetraphenyltetracene (rubrene) and coumarin 152A(481) [27]. Therefore the 0–0 energy of the S_2 transition in isolated β-Car is expected to lie at $22\,870 \pm 200$ cm^{-1} (437 ± 4 nm).

Table 1
Absorption band maxima and widths of β-Car at 295 K

Matrix	$\phi(n^2)$ [a]	$\phi(\epsilon)$ [b]	$\nu(S_{21})-22\,304$ (cm^{-1}) [c]	$\Gamma(S_{20})$ (cm^{-1}) [d]
n-pentane	0.2193	0.220	0	1207
n-hexane	0.2290	0.229	−141	
n-heptane	0.2359	0.236	−170	
n-octane	0.2410	0.240	−212	
n-decane	0.2479	0.248	−224	
n-undecane	0.2515		−314	
n-tetradecane	0.2578		−379	
n-hexadecane	0.2611		−398	1219
Diethyl ether	0.2166	0.526	−106	1285
Methyl acetate	0.2203	0.653 [e]	−234	1307
Acetone	0.2200	0.868	−272	1356
Acetonitrile	0.2119	0.924 [e]	−244	1374
PVB	0.287 [f]	0.404 [g]	−679	1458
PSt	0.338 [f]	0.339 [g]	−974	1409
CP47				1037

[a] $\phi(n^2)=(n^2-1)/(n^2+2)$; n, refractive index for Na D line at 293 K from Ref. [24].
[b] $\phi(\epsilon)=(\epsilon-1)/(\epsilon+2)$; ϵ, dielectric constant at 293 K from Ref. [24].
[c] Central peak wavenumber relative to that in *n*-pentane.
[d] First gaussian band width.
[e] At 298 K.
[f] From Ref. [25].
[g] From Ref. [26].

Table 2
Absorption band maxima and widths of Pheo *a* at 295 K

Matrix	$\nu(S_1)-14\,957$ (cm^{-1}) [a]	$\Gamma(S_1)$ (cm^{-1}) [b]	$\nu(S_2)-18\,753$ (cm^{-1}) [a]	$\Gamma(S_2)$ (cm^{-1}) [c]	ν(Soret) − 24 472 (cm^{-1}) [a]
n-pentane	0	347	0	364	0
n-hexane	−9		−12		−36
n-heptane	−14		−19		−63
n-decane	−27		−40		−131
n-hexadecane	−41		−61		−172
Diethyl ether	35	388	−2	383	20
Methyl acetate	57	430	−36	423	−22
Acetone	67	445	−40	432	−25
Acetonitrile	85	466	−62	443	−25
PVB	−7	435	−139	442	−292
RC of PS II			−303		

[a] Relative to *n*-pentane.
[b] Full width at half-maximum (FWHM).
[c] FWHM; the zero-absorption level was arbitrarily fixed at 555 nm.

Spectroscopy of photosynthetic pigments in the gas phase is a very difficult task, because of their low thermal stability and low vapour pressure. So, the 0–0 transition energies and the magnitudes of the absolute vacuum-to-matrix shifts are of considerable interest, because most quantum mechanical calculations are performed for isolated molecules or their complexes.

Another important spectroscopic parameter, the average static polarizability difference $\Delta\alpha$ between the ground and the excited state, can be estimated from the value of p (Eq. (1)) by using the Bakhshiev formula [30]:

$$\nu=\nu_0-[3\Delta\alpha\Pi'/2a^3(I+I')]\phi(n^2) \quad (2)$$

where a is the Onsager cavity radius and I and I' are the ionization potentials of the solute and solvent molecules respectively. A common value of ionization potentials (about 10 eV) for all the solvents and solutes is usually applied [30]. However, the spherical cavity radius remains a poorly defined parameter for planar and, particularly, for linear chromophores.

These difficulties can be avoided with the aid of an empirical relationship between the electrochromic $\Delta\alpha$ values and slopes p obtained for aromatic hydrocarbons [31]. In this case the relative molecular mass M is used as a measure of the cavity size [31]:

$$\Delta\alpha=-(0.4\pm1.5)-(18.2\pm1.4)\times10^{-6}pM \quad (3)$$

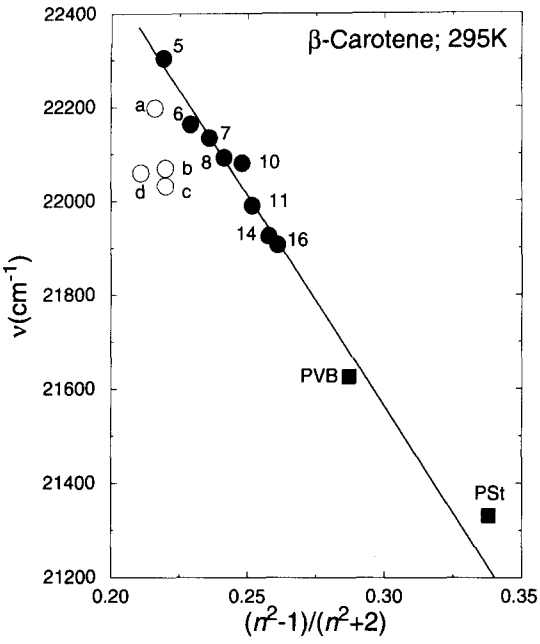

Fig. 1. Wavenumber of the central peak (S_{21}) maximum of β-Car vs. the Lorentz–Lorenz function (Eq. (1)) of the solvent at room temperature: ●, *n*-alkanes, with the number of carbon atoms indicated (5–16); ○, polar solvents (a, diethyl ether; b, methyl acetate; c, acetone; d, acetonitrile); ■, polymers (PVB, poly(vinyl butyral); PSt, polystyrene).

From Eq. (3) we estimate the polarizability changes accompanying electronic excitation to the S_1, S_2 and Soret levels of Pheo *a* as 10.0 ± 2, 16.7 ± 2 and 48 ± 7 Å^3. These values are close to the corresponding magnitudes of $\Delta\alpha$ for free base meso-tetraphenylporphine, obtained by the same method (7.6 ± 2, 18 ± 3 and 47 ± 5 Å^3) [3,31,32]. Complex formation with magnesium in Chl *a* results in an increase in $\Delta\alpha$ for the Q_y transition (18 ± 3 Å^3) and a decrease for the Soret transition (35 ± 5 Å) [3]. The solvatochromic value of $\Delta\alpha$ for β-Car (88 ± 15 Å^3) is underestimated by a factor of about 3 as compared with the estimate from electrochromic data for polyenes with 11 conjugated double bonds (including C=O): bixin methylester (223 ± 12 Å^3) and lycopene (246 ± 22 Å^3) [33]. In case of rod-shaped molecules, the effective interaction radius is obviously much larger than the size of the spherical cavity calculated from molecular weight.

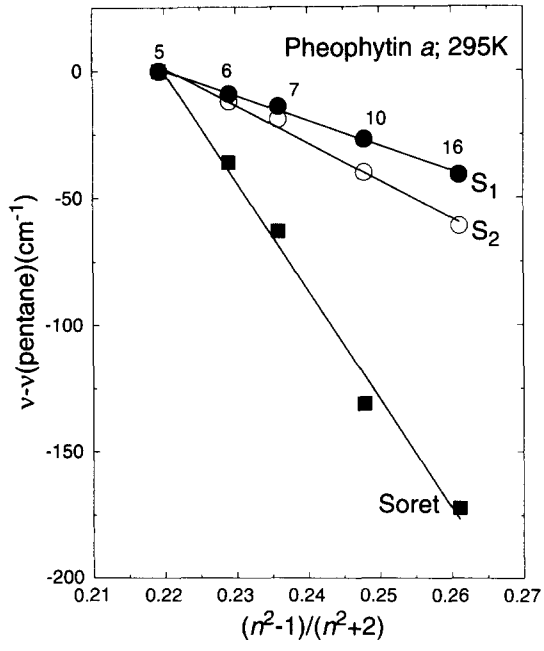

Fig. 2. Wavenumber of the peak maximum of the S_1 (Q_y) (●), S_2 (Q_x) (○) and Soret (B) (■) absorption bands of Pheo *a* vs. the Lorentz–Lorenz function (Eq. (1)) of *n*-alkanes at room temperature. The wavenumber is plotted as the difference with respect to the value found in *n*-pentane. The numbers 5, 6, 7, 10 and 16 refer to the number of carbon atoms of the *n*-alkanes.

3.2. Band shifts in polar solvents

The influence of solvent polarity was explored in a set of liquids with different dielectric permittivities ϵ but with very similar refractive indices (Table 1). A linear relationship between the band maxima and the solvent polarity function was observed (Fig. 3):

$$\nu = \nu_{0,\epsilon} + y[\phi(\epsilon) - \phi(n^2)] \quad (4)$$

in which $\phi(\epsilon) = (\epsilon - 1)/(\epsilon + 2)$. The Lorentz–Lorenz function $\phi(n^2)$ is subtracted from $\phi(\epsilon)$, because the dielectric behaviour of polar liquids is determined by the sum of orientational and electronic polarizability terms (Clausius–Mossotti equation; see Ref. [34]), and their difference can be used as a measure of (di)polarity. For the set of polar solvents used here $\phi(n^2)$ is practically constant. However, the linearity of the plot for β-Car in Fig. 3 is considerably improved when a correction is made with the aid of Eq. (1) for the small differences in dispersive shifts relative to that in *n*-pentane. The regression parameters of Eq. (4) are given in Table 3.

According to the theory developed in Ref. [28] the quadratic Stark effect in the solvent cavity field is linearly related to the polarizability difference $\Delta\alpha$ between the ground and the excited state and to the following dielectric function of the solvent:

$$f(\epsilon,n) = (\epsilon - n^2)(2\epsilon - n^2)/\epsilon(n^2+2)^2 \quad (5)$$

The function $f(\epsilon,n)$ is proportional to ϵ at high dielectric permittivities ($\epsilon \gg n^2$), whereas $\phi(\epsilon)$ approaches unity. In sets of substituted alkanes (alcohols, ketones, halogenated compounds) used predominately in Ref. [28], the polarity-dependent red shift of p bands of anthracene and tetracene is described quite well in terms of Eq. (5). However, in solvents without large non-polar hydrocarbon fragments the empirical relationship (Eq. (4)) [35] holds better.

Both dispersive and quadratic Stark shifts are expected to increase with increasing $\Delta\alpha$. Indeed, a proportionality between the slopes *p* (Eq. (1)) and *y* (Eq. (4)) was established for the S_2 transitions of Pheo *a* and β-Car as well as for the ^1L_a bands of anthracene and tetracene (Table 3):

$$y = (-21 \pm 8) + (0.0454 \pm 0.0014)p,\ r = 0.9990 \quad (6)$$

Table 3
Linear regression parameters for the dependence of absorption maxima on solvent properties (Eqs. (1) and (4))

Compound	Transition	Argument	Solvent	Intercept (cm^{-1})	Slope (cm^{-1})	N^a	$\|r\|^b$
β-Car	S_{21}	$\phi(n^2)$	*n*-alkane	24260 ± 176	−8994 ± 725	8	0.981
		$\phi(\epsilon)-\phi(n^2)$	Polar[c]	22298 ± 20	−428 ± 40	5	0.987
Pheo *a*	S_1 (Q_y)	$\phi(n^2)$	*n*-alkane	15173 ± 8	−982 ± 34	5	0.998
		$\phi(\epsilon)-\phi(n^2)$	Polar	14958 ± 5	113 ± 11	5	0.986
	S_2 (Q_x)	$\phi(n^2)$	*n*-alkane	19079 ± 18	−1477 ± 75	5	0.996
		$\phi(\epsilon)-\phi(n^2)$	Polar	18760 ± 11	−84 ± 23	5	0.903
	Soret (B)	$\phi(n^2)$	*n*-alkane	25413 ± 58	−4280 ± 243	5	0.995
		$\phi(\epsilon)-\phi(n^2)$	Polar	24481 ± 14	−50 ± 29	5	0.706
Anthracene	S_1 (^1L_a)	$\phi(n^2)$	*n*-alkane[d]	27635 ± 20	−4175 ± 85	6	0.999
		$\phi(\epsilon)-\phi(n^2)$	Polar[c,e]	26722 ± 3	−220 ± 7	5	0.999
Tetracene	S_1 (^1L_a)	$\phi(n^2)$	*n*-alkane[f]	22512 ± 50	−5137 ± 207	6	0.997
		$\phi(\epsilon)-\phi(n^2)$	Polar[c,e]	21380 ± 4	−251 ± 10	5	0.998

[a] Number of solvents.
[b] Correlation coefficient.
[c] Corrections for slightly different dispersive shift relative to *n*-pentane were introduced.
[d] Ref. [27], data from Ref. [28].
[e] Data from Ref. [28]. Solvents: *n*-pentane, diethyl ether, ethyl acetate, acetone, acetonitrile.
[f] Ref. [27], data from Ref. [29].

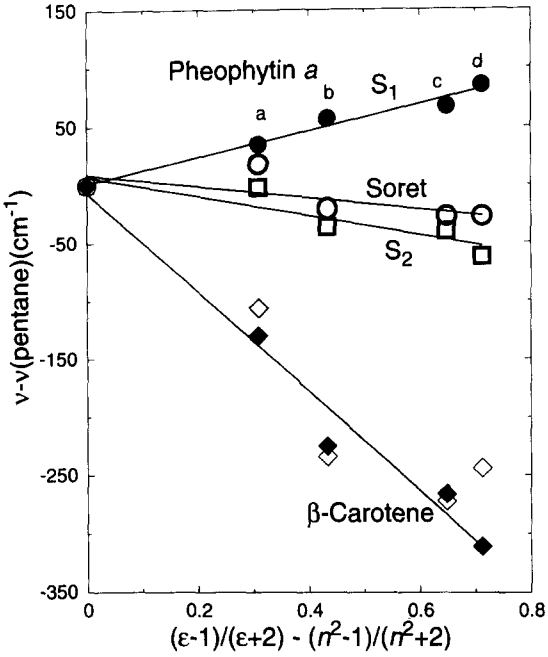

Fig. 3. Spectral shifts (relative to *n*-pentane) of β-Car (◇) and Pheo *a* S_1 (●), S_2 (□) and Soret (○) absorption bands vs. solvent polarity at room temperature. Corrections for slightly different dispersive shifts were introduced for β-Car (◆). Solvents: a, diethyl ether; b, methyl acetate; c, acetone; d, acetonitrile.

The effective cavity field E in a solvent can be estimated from the Stark shift $\Delta\nu$ and the magnitude of $\Delta\alpha$:

$$E=(2\Delta\nu/\Delta\alpha)^{1/2} \quad (7)$$

For example, in highly polar acetonitrile ($\epsilon=37.5$ at 25 °C) the β-Car molecule is subjected to a longitudinal electric field as strong as 4×10^8 V m^{-1}, which induces a dipole moment change $\Delta\mu=E\Delta\alpha/2=4.8$ D (1.64×10^{-29} C m) and a red shift of 300 cm^{-1} (6.0×10^{-21} J). In this calculation it was assumed that β-Car is similar to another polyene with 11 double bonds, lycopene, having a polarizability difference $\Delta\alpha_m=726$ Å^3 (8.1×10^{-38} C m^2 V^{-1}) in the direction of the transition moment [33].

The remarkable hypsochromic shift of the Q_y (S_1) band of Pheo *a* in polar environments cannot be understood in terms of the solvent Stark effect because the excited state has a higher polarizability than the ground state. Alternative shift mechanisms, which may result from the changes in bond dipole moments on excitation, should be considered in case of the Q_y band of Pheo *a* [32].

3.3. Spectral band widths at room temperature

FWHMs of the first Gaussian component (S_{20}) of the β-Car absorption contour as well as of the Q bands of Pheo *a* are presented in Tables 1 and 2 respectively. An increase in solvent polarity leads to band broadening, which is roughly linear with $\phi(\epsilon)-\phi(n^2)$ (Fig. 4) and has a slope y_Γ (Table 4):

$$\Gamma=\Gamma_0+y_\Gamma[\phi(\epsilon)-\phi(n^2)] \quad (8)$$

There exists some similarity between the absolute values of slopes y_Γ (Eq. (8)) (114, 164 and 231 cm^{-1}) and y (Eq. (4)) (84, 113 and 428 cm^{-1}) for S_2 and S_1 bands of Pheo *a* and β-Car respectively. Evidently, the fluctuating cavity field provides an additional broadening mechanism in polar solvents.

On the contrary, the large bandwidth of β-Car in *n*-pentane (1207 cm^{-1}) compared with that of the S_1 (347 cm^{-1}) and S_2 bands (364 cm^{-1}) of Pheo *a* originates probably from strong vibronic coupling to intramolecular modes rather than from density fluctuations of the solvent. The remarkably strong broadening for β-Car in polymers can tentatively be ascribed to the distortion of the backbone and, in particular,

Table 4
Linear regression parameters for the dependence of absorption band widths on solvent polarity (Eq. (8))

Compound	Transition	Intercept Γ_0 (cm^{-1})	Slope y_Γ (cm^{-1})	N^a	$\lvert r\rvert^b$
β-Car	$S_{20}{}^c$	1209 ± 3	231 ± 6	5	0.999
Pheo *a*	S_1 (Q_y)	346 ± 9	164 ± 18	5	0.983
	S_2 (Q_x)	361 ± 9	114 ± 19	5	0.961

[a]Number of solvents.
[b]Correlation coefficient.
[c]First gaussian band.

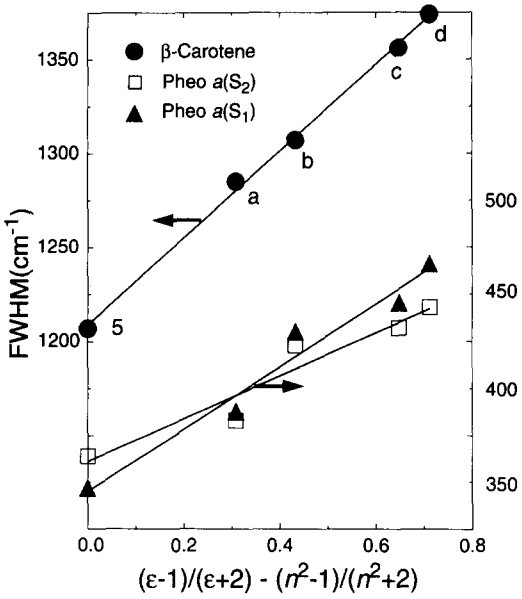

Fig. 4. Dependence of the band width of the first gaussian component of β-Car (●) and of the S_1 (▲) and S_2 (□) absorption bands of Pheo *a* at room temperature on the solvent polarity. Solvents: 5, *n*-pentane; a, diethyl ether; b, methyl acetate; c, acetone; d, acetonitrile.

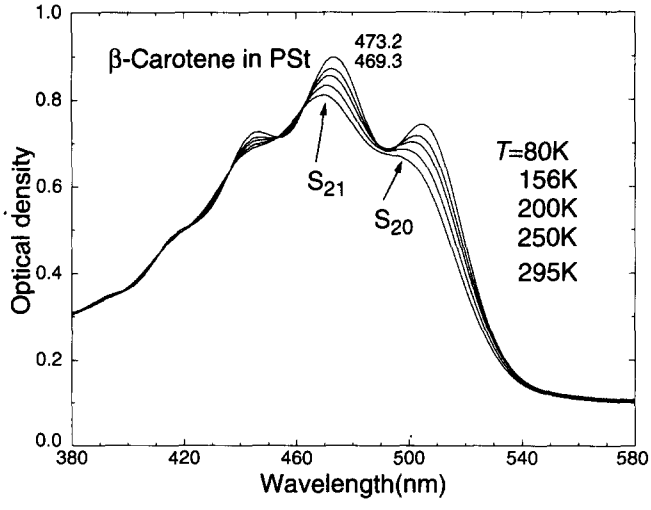

Fig. 5. Absorption spectra of β-Car in PSt at 80, 156, 200, 250 and 295 K. The peak maxima (in nanometres) for the most intense (S_{21}) band are indicated for the spectra at 80 K (upper) and at 295 K (lower).

the end rings of the flexible polyene molecule in the solid environment.

3.4. Temperature-induced band shifts in polymers

The influence of temperature on the absorption spectra of β-Car (Fig. 5) and Pheo *a* (Fig. 6) is analysed in the present and the next section. Amorphous polymers as host matrices were preferred in order to avoid the complications associated with freezing of solvents (glass transitions, cracking etc.).

Fig. 7 shows that on changing the temperature the peak maxima of the absorption bands of β-Car and Pheo *a* in polymers shift in a rather monotonic fashion. Both red shifts (β-Car and the Soret band of Pheo *a*) and blue shifts (the Q bands of Pheo *a*) are observed on cooling (Table 5).

In order to obtain an idea of the purely thermal contribution to the shift of the peak maxima, we first calculated the temperature dependence of the dispersive effect from the density and refractive index changes of the polymers. The refractive index function $\phi(n^2)$ is linearly related to the density of matter (Lorentz–Lorenz equation; see for example Ref. [34]):

$$\phi(n^2) = (4\pi N_A \alpha/3M)d \qquad (9)$$

where N_A is the Avogadro constant, α is the molecular polarizability and M is the molar mass. The density d_T/d_{293} relative to that at room temperature was obtained from tabulated values of the linear thermal expansivities a' [36]:

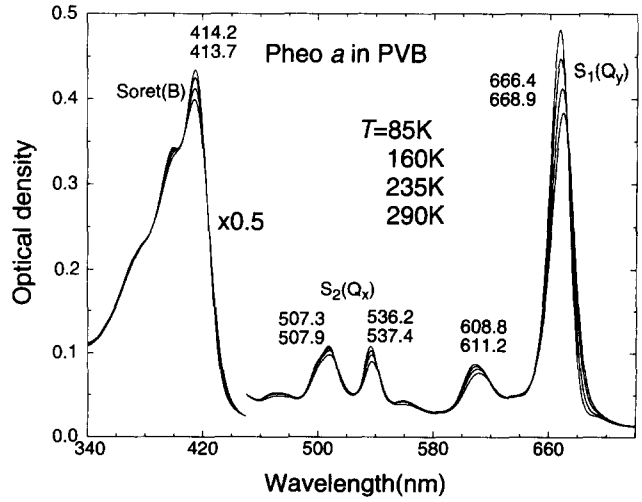

Fig. 6. Absorption spectra of Pheo *a* in PVB at 80, 160, 235 and 295 K. Peak maxima (in nanometres) are indicated for the spectra at 80 K (upper) and at 295 K (lower).

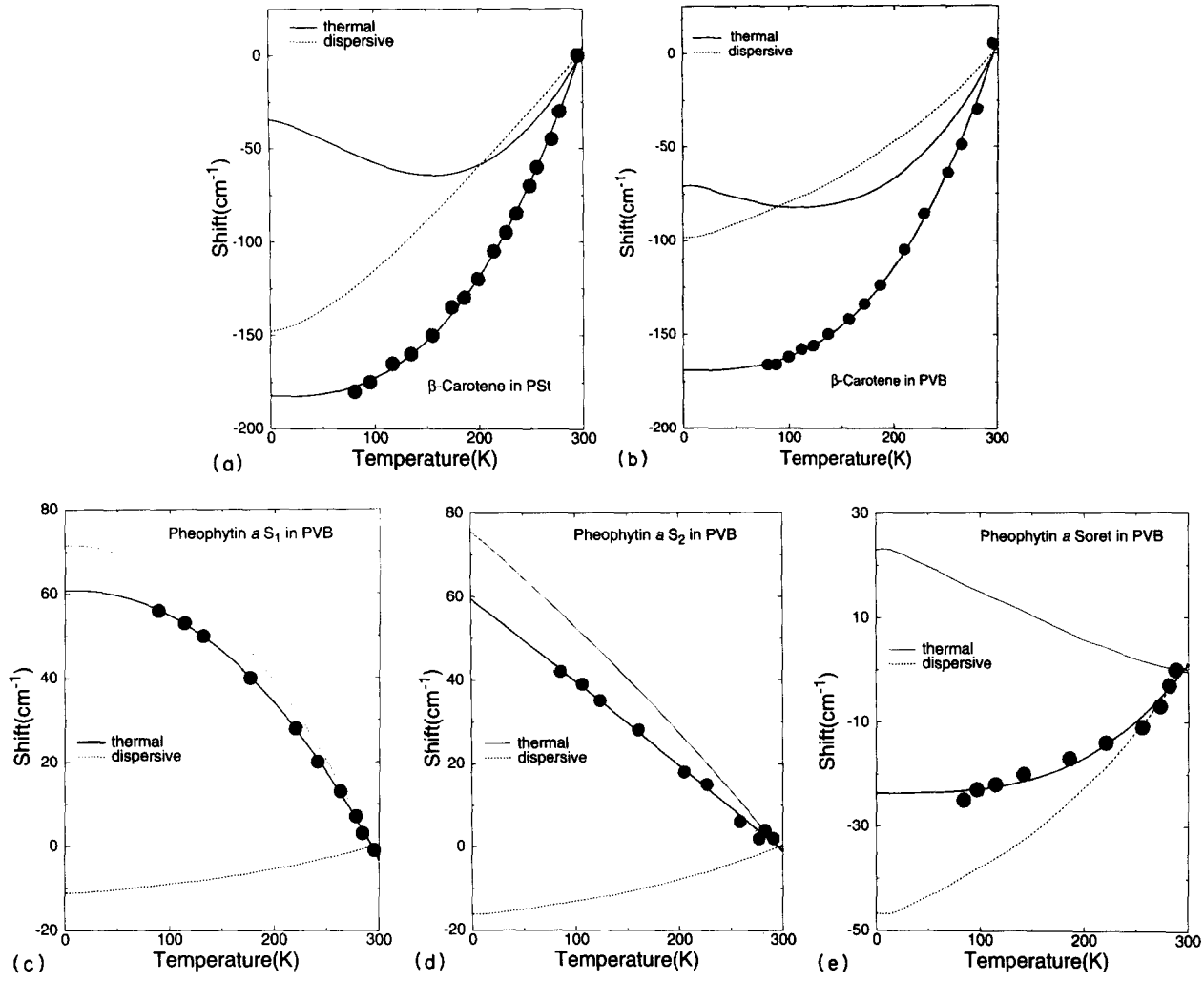

Fig. 7. Dispersive (· · · · ·) and pure thermal (———) contributions to the thermal band shifts relative to 295 K (●): (a) β-Car in PSt; (b) β-Car in PVB; (c) the S_1 (Q_y) band of Pheo *a*; (d) the S_2 (Q_x) band of Pheo *a*; (e) the Soret (B) band of Pheo *a*. The parameters of the fitting curves are given in Tables 5 and 7.

$$d_T/d_{293} = (1-a')^{-3}$$
$$a' = (l_{293} - l_T)/l_{293} \qquad (10)$$

in which l is the length of the sample.

Between 0 and 300 K the temperature dependence of d and $\phi(n^2)$ was approximated by a power law with coefficients 1.67 for PMMA and 1.34 for PSt (Table 6). Cooling the polymer down to 80 K results in a contraction of about 3%–4% (Table 6). According to Eqs. (1), (9) and (10), the

Table 5
Temperature dependence of absorption band maxima

Compound	Transition	Matrix	$\nu(80)$ (cm^{-1})[a]	$\nu(295)$ (cm^{-1})[a]	$\nu(80)$-$\nu(295)$(cm^{-1})	a (cm^{-1})[b]	b[b]	c[b]
β-Car	S_{11}	PSt	21142	21320	−178	21137	5.2×10^{-5}	2.65
		PVB	21454	21620	−166	21451	1.11×10^{-5}	2.91
	S_{10}[c]	CP47	19953	20186	−233	19953	4.3×10^{-9}	4.35
Pheo *a*	S_1 (Q_y)	PVB	15007	14950	57	15011	-3.33×10^{-4}	2.13
	S_2 (Q_x)		18650	18608	42	18667	−0.17	1.03
	Soret (B)		24148	24180	−32	24148	3.2×10^{-7}	3.18

[a]Band maxima at 80 and 295 K.
[b]Parameters of the power law fit $\nu = a + bT^c$.
[c]First gaussian component.

Table 6
Temperature dependence of density and Lorentz–Lorenz function of polymers

Polymer	Property	$x(80)$[a]	$x(295)$[a]	a[b]	$b\times10^6$[b]	c[b]
Plexiglas (PMMA)	Relative density	1.0327[c]	1	1.0375	−2.74	1.673
PVB[d]	$(n^2-1)/(n^2+2)$	0.2966	0.287[e]	0.2978	−0.786	1.673
PSt	Relative density	1.0407[c]	1	1.0489	−24.0	1.341
PSt	$(n^2-1)/(n^2+2)$	0.3518	0.338[e]	0.3545	−8.11	1.341

[a]Numerical value of the property at $T=80$ K and 295 K.
[b]Parameters of the power law fit $x=a+bT^c$.
[c]Calculated from thermal expansivity (Eq. (10)).
[d]Thermal expansivity of PVB was taken equal to that of PMMA.
[e]Ref. [25].

temperature dependence of the dispersive shift relative to that at $T=293$ K can be calculated as

$$\Delta\nu_{disp}=p\phi(n^2)[1-(1-a')^{-3}] \quad (11)$$

where $\phi(n^2)$ stands for the Lorentz–Lorenz function at room temperature and p is the regression parameter (Eq. (1)). The use of the slope p obtained for liquid n-alkanes is justified because the band positions in non-polar liquids and in solid polymers are described by a common solvatochromic plot (Fig. 1).

Dispersive stabilization of the excited state always produces a red shift on cooling as a result of compression of the matrix. Both the observed band shift (Table 5) and the calculated dispersive contribution (Table 7) were fitted to power law dependences (Fig. 7). Their difference is the purely thermal (vibronic) part of the band shift (Fig. 7, full lines; Table 7).

For Pheo *a*, the thermal effect causes a blue shift on cooling, the extent of which is the largest for the S_1 transition and the smallest for the Soret transition. In β-Car the thermal effect first leads to a red shift on cooling which changes sign below 100 K in PVB and 160 K in PSt (Figs. 7(a) and 7(b)).

π–π transitions of haem proteins [37,38] as well as Shpolskii lines of $\alpha(^1L_b)$-type transitions in pyrene derivatives with small $|p|$ values of the order of 1000–2000 cm^{-1} [39–41] display net blue shifts on cooling. Hypsochromic displacement of zero-phonon lines of d–d transitions in metal ions [42] or defect centres in ionic or covalent crystals [43] is rather a common phenomenon. Broad multiphonon bands of defect and impurity centres in ionic crystals usually exhibit the same behaviour [44,45]. These thermal shifts have been rationalized in terms of quadratic harmonic coupling, when the excited state adiabatic potential curve is shallower than that of the ground state [46].

In case of β-Car, which has a very large polarizability of the S_2 state, both the dispersive and the dipole-induced-dipole intermolecular forces are much stronger in the excited state. As a result, intermolecular vibrations have higher frequencies when the molecule is in the excited state. These quasi-local modes may play a role in β-Car above 110–160 K, when both vibronic and dispersive contributions display a red shift on decreasing the temperature. Note that linear electron–phonon coupling in the harmonic case cannot account for band shifts, because the Stokes and anti-Stokes transitions have the same probability [47].

Thermal expansiveness of polymers and molecular crystals as host matrices is much larger than that of inorganic materials, and the matrix contribution to the spectral shift becomes important. In proteins above the glass transition point and in liquids the thermal change in the density and, as a consequence, the dispersive effect are even more extensive. Therefore, the analysis of thermal band shifts requires a separation of vibronic and dispersive contributions.

Table 7
Fitting parameters of calculated dispersive (Eq. (11)) and purely thermal shifts of absorption band maxima[a]

Compound	Transition	Matrix	Shift	a (cm^{-1})[b]	b[b]	c[b]	d[b]
β-Car	S_{21}	PSt	Dispersive	−148.9	0.0729	1.341	
			Thermal	−32.5	−0.235	-8.18×10^{-4}	6.67×10^{-6}
		PVB	Dispersive	−96.7	0.00707	1.673	
			Thermal	−68.8	−0.181	5.2×10^{-6}	4.71×10^{-6}
Pheo *a*	S_1 (Q_y)	PVB	Dispersive	−10.6	7.72×10^{-4}	1.673	
			Thermal	71.4	-5.65×10^{-4}	2.068	
	S_2 (Q_x)		Dispersive	−15.9	0.00116	1.673	
			Thermal	74.8	−0.115	1.137	
	Soret (B)		Dispersive	−46.0	0.00337	1.673	
			Thermal	16.9	−0.173	0.882	

[a]Relative to 295 K. Corresponding plots are shown in Fig. 7.
[b]Parameters of the fits $a+bT^c$ or $a+bT+cT^2+dT^3$ (for the curves with a minimum).

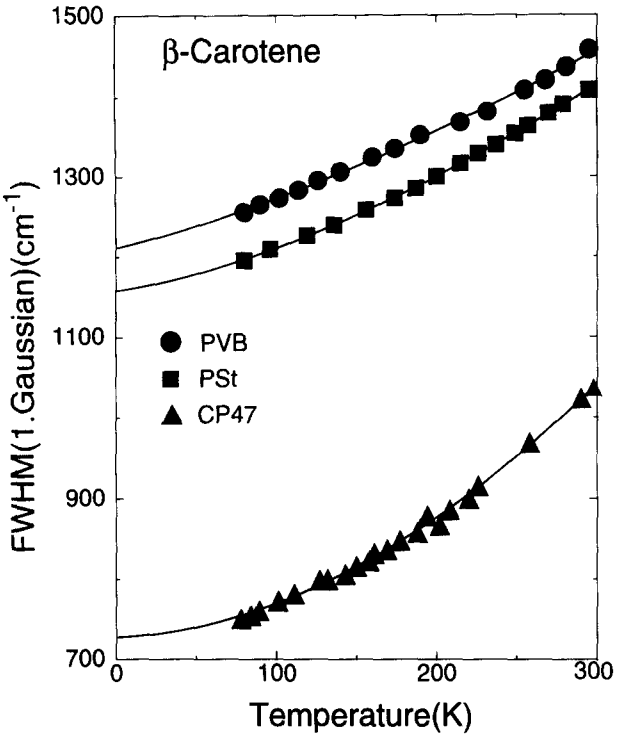

Fig. 8. Temperature dependence of the band width of the first gaussian component in the absorption spectrum of β-Car in polymers (●, ■) and in CP47 (▲). ———, fits, the parameters of which are listed in Table 7.

3.5. Temperature-induced band broadening of β-Car and Pheo α in polymers

Absorption bands of β-Car (Fig. 5) and Pheo α (Fig. 6) display remarkable narrowing on cooling. The dependence of the FWHM as a function of temperature can successfully be fitted with a power law (Figs. 8 and 9):

$$\Gamma = \Gamma_0 + aT^b \qquad (12)$$

The regression parameters Γ_0, a and b are collected in Table 8.

The widths of the first gaussian component (S_{20}) were used for β-Car. A doubled value of the HWHM of the long-wavelength side was determined for the Soret band of Pheo *a*. The background was set to zero at 555 nm to obtain the FWHM of the Q_x transition in Pheo *a*.

A nearly quadratic temperature dependence ($b = 1.5$–1.7) was established for the three investigated bands of Pheo *a*. The T^2 law dominates in a broad temperature range between 10 and 300 K in the case of zero-phonon lines in *d* and *f* ions doped into inorganic glasses [48] and crystals (above 50 K) [49] as well as in several Shpolskii systems [39,40,50,51]. Permanent hole burning in Pheo *a* in solvent glasses and polymers has revealed that nearly half of the band intensity belongs to zero-phonon transitions (Debye–Waller factor is close to 0.5) [52]. Consequently, the analogy between zero-phonon lines and the (inhomogeneously broadened) bands of Pheo *a* is meaningful at least for the S_1 transition. It should be noted that the origin of the quadratic dependence of line widths in glasses at the high temperature regime is not fully understood [53].

In contrast to the situation described above, linear electron–phonon coupling theory predicts a square root T dependence for multiphonon bands in the high temperature limit [47]. Thus, the diminishing of coefficient b in the case of β-Car may well reflect a strong coupling to low frequency modes.

In general, temperature broadening and solvent shifts are to some extent correlated. Larger values of $|p|$ (Eq. (1)) correspond to a larger absolute increase in band width between 80 and 280 K (Table 8). The magnitude of the solvent shift is related to a change in intermolecular interaction forces on electronic excitation. The latter results in a shift of the minimum and a change in the curvature of the adiabatic potential of low frequency modes, which in turn leads to an enhancement of electron–phonon coupling [54]. Also, the amplitude of both static and dynamic modulation of the transition energy as a result of density fluctuations of the matrix should increase in parallel with the solvent shift.

3.6. β-Car in CP47

CP47 is a Chl *a*–β-Car containing protein complex that is closely associated with the photochemical RC of green plant PS II. The protein is monomeric, and binds approximately 13–15 Chl *a* and 2 β-Car molecules [15,55]. A prominent feature of CP47 is that at all temperatures between 80 and 295 K the β-Car absorption bands are much narrower than those in the polymer matrices. At room temperature, the first

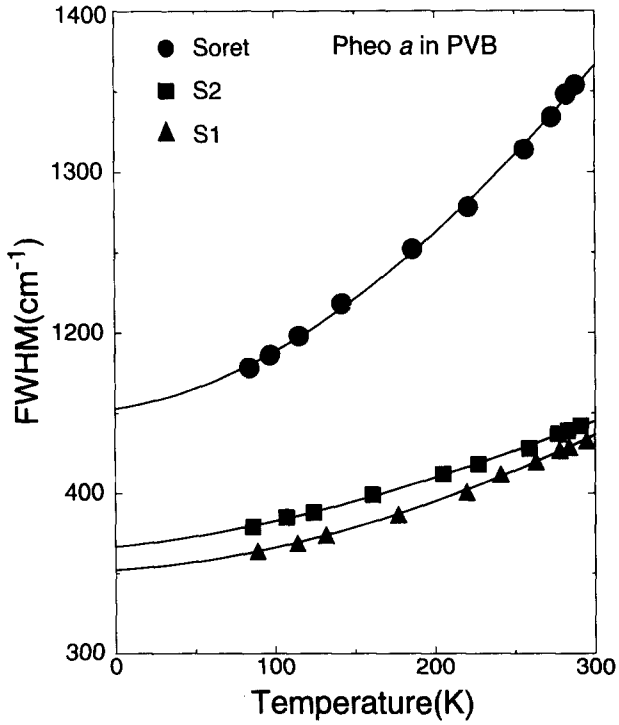

Fig. 9. Temperature dependence of the band widths of the S_1 (▲), S_2 (■) and Soret (●) absorption bands of Pheo *a* in PVB. ———, fits, the parameters of which are listed in Table 8. Note the different scaling of the *y* axis for the Soret and Q transitions.

Table 8
Temperature dependence of absorption band widths (full width at half-maximum)

Compound	Transition	Matrix	$\Gamma(80)$ (cm^{-1})[a]	$\Gamma(295)$ (cm^{-1})[a]	$\Delta\Gamma$ (cm^{-1})[b]	Γ_0 (cm^{-1})[c]	a[c]	b[c]
β-Car	S_{20}[d]	PSt	1195	1409	214	1162	0.0478	1.505
		PVB	1255	1458	203	1214	0.143	1.304
		CP47	752	1032	280	729	0.00859	1.841
Pheo *a*	S_1 (Q_y)	PVB	362	443	71	353	0.0055	1.688
	S_2 (Q_x)[e]		378	433	65	368	0.0152	1.497
	Soret (B)[f]		1177	1363	186	1155	0.0148	1.677

[a]Band widths at 80 and 295 K.
[b]Band broadening between 80 and 295 K.
[c]Parameters of the power law fit $\Gamma_0 + aT^b$.
[d]First gaussian component.
[e]Zero-absorption level was arbitrarily fixed at 555 nm.
[f]Double half-width at half-maximum (HWHM) of the red side.

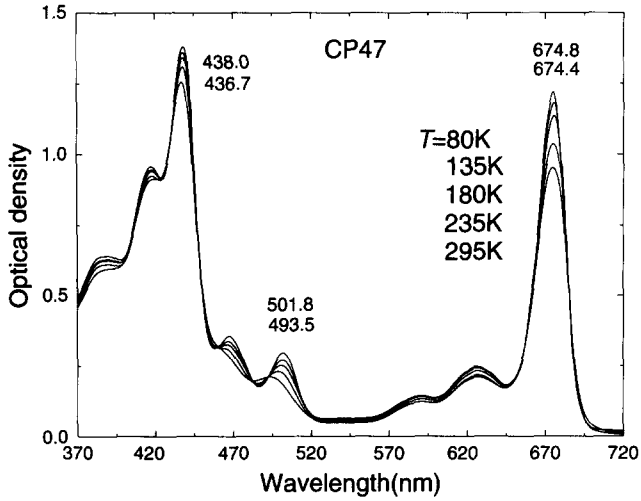

Fig. 10. Absorption spectra of CP47 in a buffer containing 70% glycerol at 80, 135, 180, 235 and 295 K. Peak maxima (in nanometres) are indicated for the spectra at 80 K (upper) and at 295 K (lower).

gaussian bandwidth is about 1037 cm^{-1}, which is even narrower than in the non-polar and weakly polarizable *n*-pentane (1207 cm^{-1}). It is evident from the simple comparison with the spectra in model environments (Table 1) that the protein pocket of β-Car should be highly ordered, even at ambient temperatures, and that the conformation of β-Car should be rigidly fixed in the protein crevice.

The peak maxima of the β-Car absorption bands (Table 1) allow one to estimate the effective refractive index value of the protein environment. Solvatochromic measurements were performed for the highest peak maximum (S_{21}) of β-Car (see Section 3.1). This maximum is not resolved in CP47 because of the overlap with the Chl *a* Soret transition at ambient temperature. The distance between the maximum of the first gaussian band and the S_{21} peak is practically independent of the band width and equals 1390 ± 20 cm^{-1} in all matrices. Thus the main maximum of β-Car should occur at 20 180 $cm^{-1} + 1390$ $cm^{-1} = 21\ 570$ cm^{-1}. The effective value of *n* as found from the solvatochromic plot for *n*-alkanes is 1.51 ± 0.04. Seferis' compilation of refractive indices [25] gives a very close number (1.539–1.541) for proteins.

This value is lower than that obtained previously for sphaeroidene in the light-harvesting LH2 complex from *Rb. sphaeroides* ($n = 1.63$) [4]. However, Stark effect experiments have demonstrated that spheroidene has a large matrix-induced dipole moment which changes considerably on excitation [56]. Correction for the Stark shift in the cavity field will decrease the value of the estimated refractive index of the LH2 protein environment. It should be noted, however, that no Stark spectra of CP47 are available, as a result of which it is not known whether local electric field effects could also have influenced the band maxima and the estimated refractive index value for CP47.

Fig. 10 shows that in CP47 between 80 and 295 K pronounced spectral changes take place in the region where the β-Car absorption dominates (between 450 and 520 nm). The peak wavelengths of the β-Car absorption bands depend strongly on temperature, and especially between 180 and 295 K the shifts are much larger in the protein complex than that

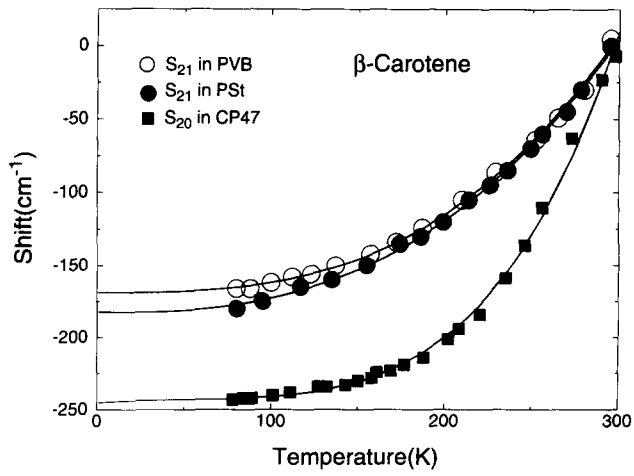

Fig. 11. Temperature-induced band shifts (relative to 295 K) of β-Car in polymers (the central peak maximum, ○, ●) and in CP47 (the first gaussian maximum, ■). ———, fits, the parameters of which are listed in Table 5.

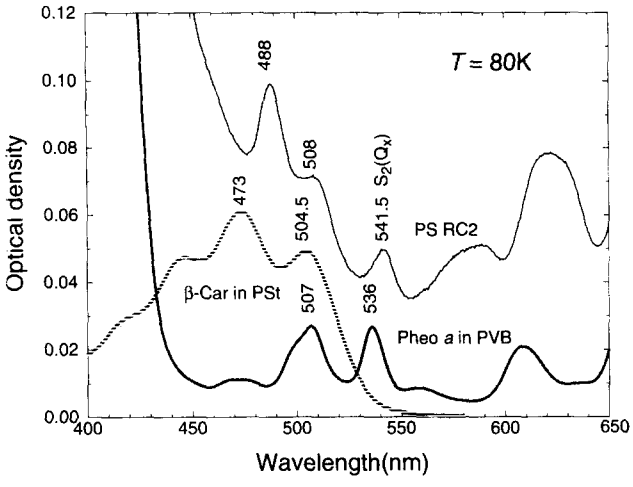

Fig. 12. Absorption spectrum at 80 K of the PS II RC complex, compared with arbitrarily scaled spectra of β-Car and Pheo *a* in polymers.

in the polymer matrices (Fig. 11 and Table 5). Also, the temperature dependence of the β-Car band width is more pronounced in CP47 than in the polymer matrices (Fig. 8 and Table 8).

It is possible that the observed temperature dependence of the peak maxima of the β-Car absorption bands in CP47 is related to the glass transition in the protein near 200 K. Several proteins have glass transitions near 200 K [57–59], suggesting that the observed temperature dependence may be related to a rapid decrease in the density of the matrix above 200 K. In other words, the protein environment could change from a solid-like medium to a liquid-like medium above 200 K. We note that about the same temperature dependence as in Fig. 11 was found for the quantum yield of chlorophyll fluorescence of the CP47 complex, which was explained by an increase in the decay rate of the excited state as a result of an increased probability of internal conversion [23].

3.7. Pheo a and β-Car in the reaction centre complex of photosystem II

The PS II RC complex prepared by a short Triton X-100 treatment [22] usually binds 6 or 7 Chl *a*, 2 Pheo *a* and 1 or 2 β-Car molecules [60]. Inspection of the absorption spectra (Fig. 12) reveals that both the Q_x band maximum of Pheo *a* (peaking at 541.5 nm at 80 K and at 542 nm at 295 K) and the absorption maxima of β-Car (488 nm at 80 K and 483 nm at 295 K) possess rather unusual positions. Possible reasons for such deviations will be discussed below.

Concerning the 542 nm (18 450 cm^{-1}) Q_x peak of Pheo *a*, the dispersive shift in a protein environment with $\phi(n^2) = 0.31–0.35$ will lower the transition energy from about 533 nm (or 18 753 cm^{-1}) in *n*-pentane to 537–539 nm (18 620 − 18 550 cm^{-1}; see Fig. 2 and Table 3). A wavelength maximum of 538 nm was indeed found for monomeric Pheo *a* in a protein–detergent–glycerol–water mixture [61], obtained by acidification of uncoupled Chl *a* from the core antenna protein CP47 [62]. The remaining red shift of 100–170 cm^{-1} can formally be ascribed to a very high polarity of the protein matrix, although the influence of the polarity on the S_2 band maximum is rather weak (Fig. 3). It is more probable that the shift reflects specific rather than universal interactions. It has, for instance, been concluded that the Pheo *a* molecule that acts as the primary electron acceptor of the PS II RC is hydrogen bonded to a glutamic acid molecule (Glu-130 of the D1 protein) [63]. Addition of 20% water to the Pheo *a* solution in acetone produces a bathochromic shift of the S_2 band from 534.5 to 535.6 nm. Much larger (440 cm^{-1} or 13 nm) displacement of the S_2 transition takes place when an excess of tris(1,1,1,2,2,3,3-heptafluoro-7,7-dimethyl-4,6-octanedionato)europium [Eu(fod)$_3$] is added to a 10^{-5} M solution of Pheo *a* in CCl_4 [64]. Thus the red shift may originate from an interaction between the isocyclic carbonyl with a proton or some other positively charged ion. Excitonic interactions between relatively weak Q_x transitions of the Pheo *a* molecules seem to be less probable.

Fig. 12 also shows that the positions of β-Car absorption bands of the PS II RC complex peak cannot be understood in terms of matrix shifts in isotropic media. Low temperature linear dichroism experiments have revealed that the peak and shoulder at 488 and 508 nm have about perpendicular orientations [22,65,66], which has been interpreted as the result of excitonic coupling between a pair of β-Car molecules [66]. The intensities of the split bands are redistributed, as expected from the simple dipole–dipole interaction model [1,67] with most of the intensity in the 488 nm band. Note that a large part of the intensity of the 508 nm shoulder must be due to the vibronic Q_x (0–1) band of Pheo *a* peaking near 512 nm (see Fig. 12). The peak position of the main band shifts from 488 nm at 80 K to 483 nm at 295 K. The extent of this shift (about 210 cm^{-1}) is somewhat smaller than that observed for β-Car in CP47 (about 250 cm^{-1}; see Fig. 11). At room temperature, the hypothetical absorption band maximum of non-interacting β-Car molecules is expected to lie just between excitonically split bands at 483 and 503 nm, i.e. 493 nm, which is about the same peak position as observed for β-Car in CP47. This suggests that the effective refractive indices for the protein environment of β-Car in CP47 and in the PS II RC complex should be about the same.

4. Conclusions

Salient features of pigment–protein complexes such as the presence of permanent local electric fields, the well-defined microenvironment of the chromophore and the resonant interaction between the pigments cannot be mimicked in isotropic solutions. However, a rather detailed study of pigments in liquids and polymers allows one to discern peculiarities of the protein environment.

In this work the spectral properties of β-Car and Pheo *a* have been compared with those in functional photosynthetic complexes of PS II. Temperature-induced shifts of absorption band maxima in polymers have been divided into two parts:

the dispersive and the purely thermal (vibronic) contributions. Provided that the vibronic contribution is known, the absorption band maxima can serve as probes of the local density (polarizability, compressibility, thermal expansion coefficient) of proteins.

The effective value of the refractive index of the medium surrounding β-Car in CP47 at room temperature was found to be 1.51 ± 0.04. A high degree of local order of the crevice housing β-Car at ambient temperature can be recognized on the basis of the observed small band width (less than in *n*-alkanes).

The primary electron acceptor Pheo *a* in the RC of PS II is probably imbedded in a special environment, which leads to an extra bathochromic shift of the Q_x band. Displacement and distortion of the β-Car absorption profile in the RC of PS II can be preferably rationalized in terms of excitonic coupling, rather than by assuming unrealistic polarizabilities and local fields of the host matrix.

Acknowledgements

We thank Dr. Tõnu Pullerits for useful discussions of vibronic coupling problems and for the help in data processing. I.R. was supported by a visiting fellowship from the Netherlands Organization for Scientific Research (NWO). This research was furthermore supported by the Netherlands Foundation for Chemical Research (SON), and by the EC, Contract CT 940619.

References

[1] R.M. Pearlstein, in H. Scheer (ed.), *Chlorophylls*, CRC Press, Boca Raton, FL, 1991, p. 1047.
[2] I.V. Renge and E.V. Bitova, *Biofizika, 32* (1987) 373 (*Biophysics, 32* (1987) 403).
[3] I. Renge, *J. Phys. Chem., 97* (1993) 6582.
[4] P.O. Andersson, T. Gillbro, L. Ferguson and R.J. Cogdell, *Photochem. Photobiol., 54* (1991) 353.
[5] A.L. Lerosen and C.E. Reid, *J. Chem. Phys., 20* (1952) 233.
[6] A.B. Myers and R.R. Birge, *J. Chem. Phys., 73* (1980) 5314.
[7] H. Torii and M. Tasumi, *J. Chem. Phys., 98* (1992) 3697.
[8] T. Noguchi, H. Hayashi, M. Tasumi and G.H. Atkinson, *J. Phys. Chem., 95* (1991) 3167.
[9] W. Liptay, *Z. Naturforsch., Teil A, 20* (1965) 1441.
[10] A.R. Mantini, M.P. Marzocchi and G. Smulevich, *J. Chem. Phys., 91* (1989) 85.
[11] C.K. Chan and J.B. Page, *J. Chem. Phys., 79* (1983) 5234.
[12] Z.Z. Ho, R.C. Hanson and S.H. Lin, *J. Chem. Phys., 77* (1982) 3414.
[13] W. Siebrand and M.Z. Zgierski, *J. Chem. Phys, 71* (1979) 3561.
[14] O. Nanba and K. Satoh, *Proc. Natl. Acad. Sci. USA, 84* (1987) 109.
[15] H.-C. Chang, R. Jankowiak, C.F. Yocum, R. Picorel, M. Alfonso, M. Seibert and G.J. Small, *J. Phys. Chem., 98* (1994) 7717.
[16] A. Gorokhovskii, V. Korrovits, V. Palm and M. Trummal, *Chem. Phys. Lett., 125* (1986) 355.
[17] K.K. Rebane and A.A. Gorokhovskii, *J. Lumin., 36* (1987) 237.
[18] K.-P. Müller and D. Haarer, *Phys. Rev. Lett., 66* (1991) 2344.
[19] G. Schulte, W. Grond, D. Haarer and R. Silbey, *J. Chem. Phys., 88* (1988) 679.
[20] S. Völker, *Annu. Rev. Phys. Chem., 40* (1989) 499.
[21] J.P. Dekker, N.R. Bowlby and C.F. Yocum, *FEBS Lett., 254* (1989) 150.
[22] S.L.S. Kwa, W.R. Newell, R. Van Grondelle and J.P. Dekker, *Biochim. Biophys. Acta, 1099* (1992) 193.
[23] M.-L. Groot, E.J.G. Peterman, I.H.M. Van Stokkum, J.P. Dekker and R. Van Grondelle, *Biophys. J., 68* (1995) 281.
[24] A.J. Gordon and R.A. Ford, *The Chemist's Companion*, Wiley, New York, 1972. *Aldrich Catalog Handbook of Fine Chemicals 1988–1989*, Aldrich Chemical Company, Milwaukee, WI, 1988. A.I Koppel and V.A. Palm, in N.B. Chapman and J. Shorter (eds.), *Advances in Linear Free Energy Relationships*, Plenum, London, 1972. p. 203. J.A. Riddick and N.B. Bunger, *Organic Solvents. Physical Properties and Methods of Purification*, Vol. II, Wiley, New York, 1970.
[25] J.C. Seferis, in J. Brandrup and E.H. Immergut (eds.), *Polymer Handbook*, Wiley, New York, 3rd edn., 1989, p. VI/451.
[26] R.B. Altmann, I. Renge, L. Kador and D. Haarer, *J. Chem. Phys., 97* (1992) 5316.
[27] I. Renge, *J. Photochem. Photobiol. A: Chem., 69* (1992) 135.
[28] M. Nicol, J. Swain, Y.-Y. Shum, R. Merin and R.H.H. Chen, *J. Chem. Phys., 48* (1968) 3587.
[29] O.E. Weigang, Jr. and D.D. Wild, *J. Chem. Phys., 37* (1962) 1180.
[30] N.G. Bakhshiev, O.P. Girin and I.V. Piterskaya, *Opt. Spektrosk., 24* (1968) 901 (*Opt. Spectrosc., 24* (1968) 483).
[31] I. Renge, *Chem. Phys., 167* (1992) 173.
[32] I. Renge, *Chem. Phys. Lett., 185* (1991) 231.
[33] K. Seibold, H. Navangul and H. Labhart, *Chem. Phys. Lett., 3* (1969) 275.
[34] C.J.F. Böttcher, *Theory of Electric Polarization, Vol. I*, Elsevier, Amsterdam, 1973.
[35] P. Suppan, *J. Photochem. Photobiol. A: Chem., 50* (1990) 293.
[36] *Landolt-Börnstein. Zahlenwerte und Funktionen*, Vol. II, Part I, Springer, Berlin, 6th edn., 1971, p. 710.
[37] L. Cordone, A. Cupane, M. Leone and E. Vitrano, *Biophys. Chem., 24* (1986) 259.
[38] A. DiPace, A. Cupane, M. Leone, E. Vitrano and L. Cordone, *Biophys. J., 63* (1992) 475.
[39] R.I. Personov and V.V. Solodunov, *Fiz. Tverd. Tela, 10* (1968) 1848 (*Sov. Phys. Solid State, 10* (1968) 1454).
[40] V.A. Kizel and M.N. Sapozhnikov, *Phys. Status Solidi, 41* (1970) 207.
[41] A.I. Laisaar, A.K.-I. Mugra and M.N. Sapozhnikov, *Fiz. Tverd. Tela, 16* (1974) 1155 (*Sov. Phys. Solid State, 16* (1974) 741).
[42] G.F. Imbusch, W.M. Yen, A.L. Schawlow, D.E. McCumber and M.D. Sturge, *Phys. Rev. A, 133* (1964) 1030.
[43] A. Halperin and O. Nawi, *J. Phys. Chem. Solids, 28* (1967) 2175.
[44] W. Gebhardt and H. Kühnert, *Phys. Status Solidi, 14* (1966) 157.
[45] G. Baldini, E. Mulazzi and N. Terzi, *Phys. Rev. A, 140* (1965) 2094.
[46] I.S. Osad'ko, in V.M. Agranovich and R.M. Hochstrasser (eds.), *Spectroscopy and Excitation Dynamics of Condensed Molecular Systems*, North-Holland, Amsterdam, 1983, p. 437.
[47] J.J. Markham, *Rev. Mod. Phys., 31* (1959) 956.
[48] W.M. Yen and R.T. Brundage, *J. Lumin., 36* (1987) 209.
[49] J. Hegarty and M.W. Yen, *Phys. Rev. Lett., 43* (1979) 1126.
[50] E.I. Al'shits, E.D. Godyaev and R.I. Personov, *Fiz. Tverd. Tela, 14* (1972) 1605 (*Sov. Phys. Solid State, 14* (1972) 1385).
[51] J.L. Richards and S.A. Rice, *J. Chem. Phys., 54* (1971) 2014.
[52] I. Renge, unpublished results, 1994.
[53] D.L. Huber, *J. Lumin., 36* (1987) 327.
[54] I. Renge, *J. Opt. Soc. Am. B, 9* (1992) 719.
[55] S.L.S. Kwa, P.J.M. Van Kan, M.L. Groot, R. Van Grondelle, C.F. Yocum and J.P. Dekker, in N. Murata (ed.), *Research in Photosynthesis, Vol. I*, Kluwer, Dordrecht, 1992, p. 263.
[56] D.S. Gottfried, M.A. Steffen and S.G. Boxer, *Biochim. Biophys. Acta, 1059* (1991) 76.
[57] F. Parak, E.N. Frolov, R.L. Mössbauer and V.I. Goldanskii, *J. Mol. Biol., 145* (1981) 825.

[58] W. Doster, S. Cusack and W. Petry, *Nature (London), 337* (1989) 754.
[59] Y. Miyazaki, T. Matsuo and H. Suga, *Chem. Phys. Lett., 213* (1993) 303.
[60] C. Eijckelhoff and J.P. Dekker, *Biochim. Biophys. Acta, 1231* (1995) 21.
[61] S.L.S. Kwa, N.T. Tilly, C. Eijckelhoff, R. Van Grondelle and J.P. Dekker, *J. Phys. Chem., 98* (1994) 7712.
[62] S.L.S. Kwa, S. Völker, N.T. Tilly, R. Van Grondelle and J.P. Dekker, *Photochem. Photobiol., 59* (1994) 219.
[63] P. Moënne-Loccoz, B. Robert and M. Lutz, *Biochemistry, 28* (1989) 3641.
[64] L.L. Shipman, T.M. Cotton, J.R. Norris and J.J. Katz, *J. Am. Chem. Soc., 98* (1976) 8222.
[65] R.J. Van Dorssen, J. Breton, J.J. Plijter, K. Satoh, H.J. Van Gorkom and J. Amesz, *Biochim. Biophys. Acta, 893* (1987) 267.
[66] W.R. Newell, H. Van Amerongen, J. Barber and R. Van Grondelle, *Biochim. Biophys. Acta, 1057* (1991) 232.
[67] R. Van Grondelle, J.P. Dekker, T. Gillbro and V. Sundström, *Biochim. Biophys. Acta, 1187* (1994) 1.